

Manuscript version: Author's Accepted Manuscript

The version presented in WRAP is the author's accepted manuscript and may differ from the published version or Version of Record.

Persistent WRAP URL:

<http://wrap.warwick.ac.uk/126046>

How to cite:

Please refer to published version for the most recent bibliographic citation information. If a published version is known of, the repository item page linked to above, will contain details on accessing it.

Copyright and reuse:

The Warwick Research Archive Portal (WRAP) makes this work by researchers of the University of Warwick available open access under the following conditions.

Copyright © and all moral rights to the version of the paper presented here belong to the individual author(s) and/or other copyright owners. To the extent reasonable and practicable the material made available in WRAP has been checked for eligibility before being made available.

Copies of full items can be used for personal research or study, educational, or not-for-profit purposes without prior permission or charge. Provided that the authors, title and full bibliographic details are credited, a hyperlink and/or URL is given for the original metadata page and the content is not changed in any way.

Publisher's statement:

Please refer to the repository item page, publisher's statement section, for further information.

For more information, please contact the WRAP Team at: wrap@warwick.ac.uk.

Unballanced Performance of Parallel Connected Large Format Lithium Ion Batteries for Electric Vehicle Application

Elham Hosseinzadeh
WMG, University of Warwick
Warwick, United Kindgdom
e.hosseinzadeh@warwick.ac.uk

Maria Ximena Odio
Jaguar and Land Rover
Warwick, United Kindgdom
modionar@jaguarlandrover.com

James Marco
WMG, University of Warwick
Warwick, United Kindgdom
james.marco@warwick.ac.uk

Paul Jennings
WMG, University of Warwick
Warwick, United Kindgdom
paul.jennings@warwick.ac.uk

Abstract— The integration of cells that exhibit differing electrical characteristics, such as variations in energy capacity and internal resistance can degrade the overall performance of the energy storage system (ESS) when those cells are aggregated into single battery pack. When cells are connected electrically in parallel, such variations can lead to significant individual differences in battery load current, state of charge (SOC) and heat generation. Further, if consideration is given to small variations in cell interconnection resistance, the detrimental effect on load imbalance is amplified. Given that cell resistance is known to be a function of both SOC and temperature, the impact of the imbalance is compounded as the performance of cells further diverge under load. During extended periods of excitation, variations in cell depth of discharge (DOD) and the occurrence of temperature gradients across the parallel connection will accelerate cell ageing and, if unmanaged, may present safety concerns such as the onset of thermal runaway. In this paper the impact of varied SOC and temperature on the overall performance of the ESS with parallel connected cells has been investigated. The results highlight that 8% variation in the initial SOC can result in a current difference of 62% among the cells, while a temperature variation of 8°C results in a current deviation of 14%. Moreover, it was found that the interconnection resistance can significantly increase the inhomogeneity.

Keywords— *Unbalanced Performance, Parallel Connected Cells, Co-Simulation, Large Format Cells, Battery Pack*

I. INTRODUCTION

Lithium ion batteries have become the dominant battery technology for automotive industry due to their high energy density, high power density, long life time and excellent storage capabilities [1]. The main concerns regarding lithium ion batteries are cost, life time, reliability and safety [2]. The performance of electric vehicles (EVs) is mainly dependent on a battery pack rather than a single cell, as an ESS includes a high number of cells connected in series and parallel [3,4]. Manufacturing inconsistencies, cells arrangements within a pack, electrical connections, control and thermal management may cause performance inconsistency between the individual cells of an ESS. This may lead to rapid ageing, capacity loss and safety concerns [1, 5-7]. The current battery management systems (BMS) do not consider variations of state of health (SOH) and SOC within the parallel cells, as they have a common terminal voltage. However this assumption may result in further degradation and over-charging/discharging hazards for individual cells [2,8].

Wu et al. [7], developed a Pseudo Two-Dimensional (P2D) electrochemical-thermal model to investigate unequal loads in a 12 parallel 7 series (12P 7S) battery pack as a result of interconnection resistance between parallel cells. They observed a significant temperature variation within the pack under different drive cycles. Bruen et al. [8], employed an equivalent circuit model (ECM) to explore the issues emerged within parallel cells in a 4P 1S module as a result of varied properties. They found out that cells with different impedances and capacities experience significantly different currents. The impact of parallel string on pack performance has been neglected for many years and it has recently been identified as one of the critical areas. Only a few studies so far have looked into the imbalanced scenarios, and developed battery pack models based on series-parallel configuration of battery cells in a pack. The previous studies employed a simplified cell model with a constant resistance, moreover the temperature dependency of the electrochemical parameters have been neglected in most cases. This research develops a combined electrical model of a parallel string with an electrochemical-thermal model of a cell to underpin a novel battery model which can be employed for designing a battery pack as well as thermal management systems. An experimentally validated 1D electrochemical-thermal model of a cell is employed to underpin the performance evaluation of parallel connected cells within the context of a complete ESS. The cell model, developed within COMSOL Multiphysics is coupled with the electrical model of the ESS within Matlab. The Results presented, quantify cell-to-cell variations in terms of internal resistance, load current, temperature and SOC as a result of discrepancy of the initial conditions and interconnection resistance. This paper is structured as follows, Section II explains the concept of the electrochemical-thermal modelling of the cell. Section III outlines the ESS electrical model. The numerical coupling between Matlab and COMSOL and the flowchart of the model operation are presented in Section IV. Section V presents the results. Further work and conclusions are discussed in Sections VI and VII respectively.

II. ELECTROCHEMICAL-THERMAL MODEL

This study focuses on variation of initial SOC's and temperatures of the cells within a parallel string on the overall performance of the pack. The various case studies are defined within Table I, and they will be elaborated in Section V. T_{0cell_i} , refers to the initial temperature of the Cell_{*i*} and *i* is the

cell number, $1 < i < 5$. Likewise, $SOC_{0,cell_i}$, is the initial SOC of the Cell_{*i*}. The following sections will focus on the modelling of the single cell as well as the electrical connection of the cells in the format of an ESS.

A 1-D electrochemical-thermal model based on the Pseudo Two-Dimensional (P2D) battery model was developed in COMSOL Multiphysics [9-11] and validated over a wide range of experiments for a large format 53 Ah commercial pouch cell with LiNixMnyCo1-x-yO2 (NMC) chemistry manufactured by Xalt Energy. The 1-D model includes one electrode pair, i.e., negative current collector, negative electrode, separator, positive electrode and positive current collector. In the 1-D model the variation of the electrochemical parameters through the thickness of the cell has been considered only, and since it is coupled with a 1-D thermal model, the temperature dependency of the parameters has been taken into account. The experiments conducted for identifying the physical parameters of the cell include, battery tear-down to quantify the number of layers, the thickness and the dimensions of each layer, along with scanning electron microscopy (SEM) for measuring the particle sizes of anode and cathode. Open circuit voltage (OCV) measurements and capacity tests under different operating conditions at 5-45°C ambient temperature were undertaken to define the dynamic parameters of the cell such as, reaction rates ($k(m^{2.5} mol^{-0.5} S^{-1})$) and the activation energies ($E_{act}(J/mol)$) for temperature dependent parameters within the Arrhenius function. The developed model was extensively validated against constant charge (0.5C-5C) and discharge (0.5-5C), moreover WLTP class 3 drive cycle (which is a gentle drive cycle for high power vehicles) as well as a high performance duty cycle [12,13], at 5-45°C. The battery surface temperature was measured by a FLIR T440 thermal camera during the experiments. Generally a battery generates heat over the course of its operation due to the reaction, ohmic and concentration polarisation. The temperature evolution of a battery is in fact the response of the battery to the heat generation. In absence of active cooling, the heat is only dissipated through natural convection from the surface of the battery as a result of the temperature difference between the battery surface and the environment. Generally it is hard to measure the heat transfer coefficient ($h (W/(m^2.K))$). However it can be estimated by quantifying the generated heat in the cell and measuring the cell temperature experimentally. In this study a natural convection boundary condition with h value of $6 (W/(m^2.K))$, provided the best fit to the experimental data. The details can be found in [11,14]. All the experiments undertaken in this study were conducted on three new cells placed in a Weiss Gallenkamp Votsch V3 4060 thermal chamber horizontally. The temperature of the thermal chamber was controlled by an electric fan. The cells were connected to a commercial cycler namely a Bitrode MCV 16-100-5 to perform the test protocols. The experimental results on the single cells, revealed a very low variation between the cells in terms of capacity and terminal voltage, with maximum 2.7% deviation in achievable capacity which can be attributed to manufacturing inconsistency, measurement error or location of the cells within the thermal chamber. Generally the manufacturing inconsistencies is higher for the cell impedances rather than the capacities and as reported within

the literature it is more likely to cause inhomogeneous current distributions [15-17].

TABLE I. CASE STUDIES FOR ESS WITH DIFFERENT INITIAL CONDITIONS.

Case studies	$T_{0,cell_1}$	$T_{0,cell_2}$	$T_{0,cell_3}$	$T_{0,cell_4}$	$T_{0,cell_5}$	R_{IC}/R_{cell}
	$SOC_{0,cell_1}$	$SOC_{0,cell_2}$	$SOC_{0,cell_3}$	$SOC_{0,cell_4}$	$SOC_{0,cell_5}$	
Test case 1	33°C	31°C	29°C	27°C	25°C	0
	1	1	1	1	1	
Test case 2	33°C	31°C	29°C	27°C	25°C	0.1
	1	1	1	1	1	
Test case 3	25°C	25°C	25°C	25°C	25°C	0
	1	0.98	0.96	0.94	0.92	
Test case 4	25°C	25°C	25°C	25°C	25°C	0.1
	1	0.98	0.96	0.94	0.92	

III. ELECTRICAL MODEL

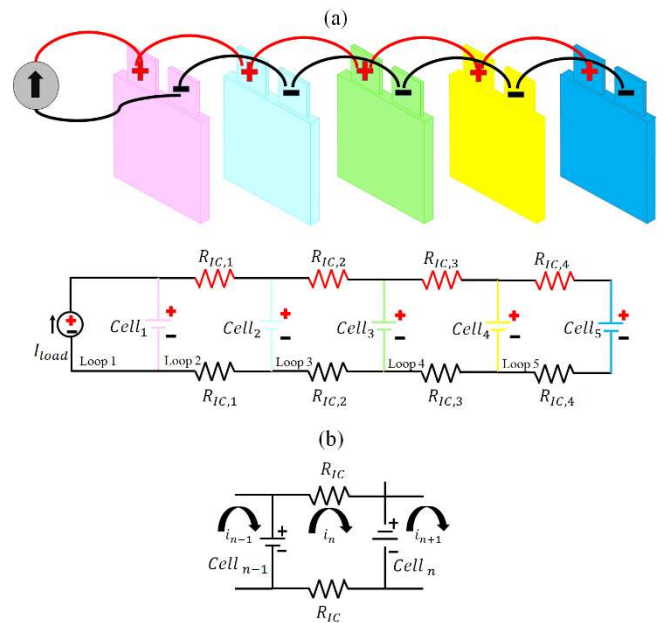


Figure 1. (a) Schematic of a battery pack with (1S 5P) configuration, showing the interconnect resistances under an applied current source, (b) Current loop for cell n , adopted from [14].

A single cell model cannot be the representative of an ESS, as arrangement of the cells within a pack, initial conditions of the cells, variation in resistance, capacity or any other parameters due to manufacturing inconsistency or system operation, highly impact the ESS behaviour. Variations in the cells parameters or initial conditions lead to a mismatch in the internal resistances which in turn forces the cells to draw different currents. It means that the cells develop different SOC and temperature over the time and they will eventually age differently. Therefore, it is very important to investigate the interaction of the cells within a pack to understand the main sources which contribute to the imbalanced performance. The ESS used in this study comprises five 53 Ah cells in parallel, which can provide a nominal capacity 265 Ah ($5 \times 53 \text{ Ah} = 265 \text{ Ah}$). The EV systems typically run at 350-400 V. Hence, the nominal energy of the ESS comprising 5

cells in parallel is around 92-106 kWh, which is enough to run a large EV ($265 \text{ Ah} \times 350\text{-}400$)/1000 = 92-106 kWh. An ESS can be represented by an electrical model. A schematic of a (1S 5P) ESS, consisting five, 53 Ah cells in parallel is presented in Figure 1. The external load is applied as a current source (I_{load}). The first cell (Cell₁) is connected to the terminals of the ESS with the remainder of cells (Cell₂₋₅) connected together via a network of resistances ($R_{IC,n}$). The characteristics of the cells are represented by a high fidelity electrochemical-thermal model. Based on Kirchoff's current law, the sum of the currents at each junction equals zero. Therefore the correlation between load current and current through each cell is defines as follows (shown in Figure 1(b)):

$$I_{cell,n} = \begin{cases} I_n - I_{n+1}, & n < N \\ I_n, & n = N \end{cases} \quad (1)$$

Similarly, from Kirchoff's voltage law, the voltages around each loop must sum to zero.

$$V_{t,n} - V_{t,n-1} + 2R_{IC}I_n = 0 \quad (2)$$

Where N represents the total number of cells in a parallel string. The terminal voltage of the cells can be expressed by:

$$V_t = OCV + R_{cell} I_{cell} \quad (3)$$

By substituting the terminal voltage (i.e. (3)) in (2), the correlation between the loop current and external load can be evaluated as:

$$\begin{bmatrix} I_1 \\ I_2 \\ I_3 \\ I_4 \\ I_5 \end{bmatrix} = [R]^{-1}([A] OCV + [B] I_{load}) \quad (4)$$

$$A = \begin{bmatrix} 0 & 0 & 0 & 0 & 0 \\ -1 & 1 & 0 & 0 & 0 \\ 0 & -1 & 1 & 0 & 0 \\ 0 & 0 & -1 & 1 & 0 \\ 0 & 0 & 0 & -1 & 1 \end{bmatrix}, B = \begin{bmatrix} 1 \\ -R_{cell1} \\ 0 \\ 0 \\ 0 \end{bmatrix}$$

$$R =$$

$$\begin{bmatrix} 1 & 0 & 0 & 0 & 0 \\ 0 & -(R_{cell1} + R_{cell2} + 2R_{IC}) & R_2 & 0 & 0 \\ 1 & R_2 & -(R_{cell2} + R_{cell3} + 2R_{IC}) & 0 & 0 \\ -1 & 1 & R_3 & 0 & 0 \\ 0 & 0 & 0 & R_4 & 0 \\ 0 & 0 & 0 & 0 & 0 \\ - (R_{cell3} + R_{cell4} + 2R_{IC}) & R_4 & - (R_{cell4} + R_{cell5} + 2R_{IC}) & 0 & 0 \end{bmatrix}$$

Where OCV is the open circuit voltage, R_{cell} is the internal resistance of the cell and R_{IC} stands for the interconnection resistance between the cells. The generalised form of the model for variable number of batteries is given by (5) and (6). The subscripts (i, j) define the matrix row and

column respectively. The terms $R_{i,j}$ and $A_{i,j}$ are representative for non-zero arrays in the respective ($n \times n$) R and A matrices.

$$\begin{cases} R_{i,j} = 1, & i = j = 1 \\ -(R_{cell(i-1)} + R_{cell(i)} + 2R_{IC}), & i = j, i > 2 \\ R_{cell(\max(i,j)-1)}, & |i - j| = 1 \end{cases} \quad (5)$$

$$A_{i,j} = \begin{cases} 1, & i > 2, i = j \\ -1, & i > 2, i - j = 1 \end{cases} \quad (6)$$

IV. NUMERICAL COUPLING BETWEEN ELECTROCHEMICAL AND ELECTRICAL MODEL

The cells in an ESS will not behave similarly, due to either manufacturing inconsistency or being exposed to various operation conditions. Therefore, in order to capture the cell to cell variation of the parallel string within an ESS, the electrical connection of the cells has to be implemented in the pack model. The underpinning electrical equations has been developed in Matlab software package. As discussed in Section II, the cell model constitutes a high fidelity electrochemical-thermal model which takes into consideration the temperature dependency of the electrochemical parameters. As defined within the flowchart in Figure 2, through a process of co-simulation, the two models are numerically coupled to form the complete ESS model. The order of the simulation process has been displayed in the flowchart within Figure 2.

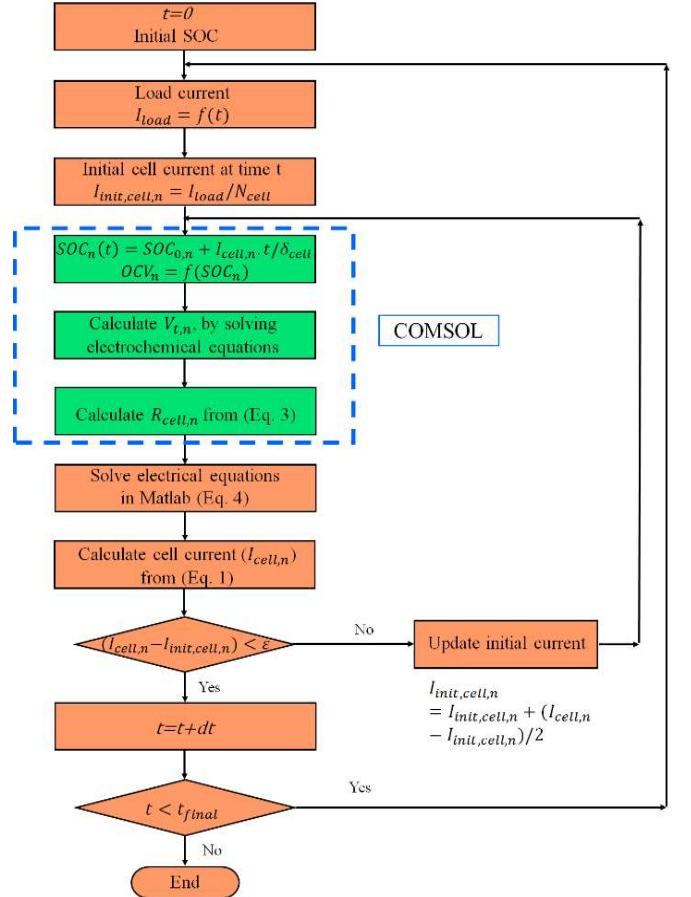


Figure 2. The flowchart of the Matlab-COMSOL co-simulation, adopted from [14].

V. RESULTS AND DISCUSSION

The performance of an ESS is dependent on both the architecture of the cells and operational conditions. Generally a higher current load increases the variations across the parallel cells and the impact is amplified as the length of the parallel connection increases [14]. This study focusses only on the impact of initial conditions on the ESS performance. All the simulations were performed at 3C continuous discharge condition. The reason for choosing a constant discharge instead of a drive cycle is to reduce the computational time.

A. Initial Temperature Variation

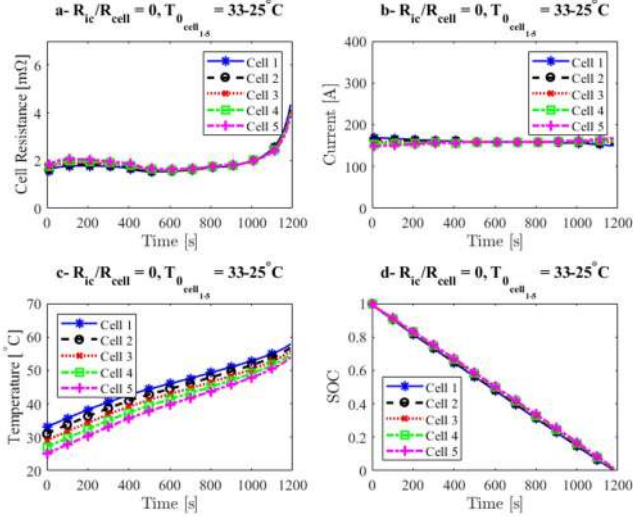


Figure 3. Resistance, current, temperature and SOC of the cells within the (1S 5P) ESS during a constant 3C discharge process due to cell to cell variation of the initial temperature, $R_{IC}/R_{cell} = 0$.

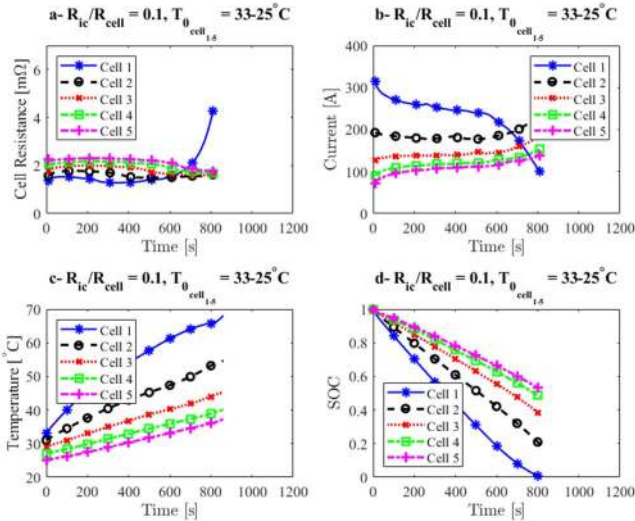


Figure 4. Resistance, current, temperature and SOC of the cells within the (1S 5P) ESS during a constant 3C discharge process due to cell to cell variation of the initial temperature, $R_{IC}/R_{cell} = 0.1$.

For an ideal case the cells will have identical properties such as resistance and capacity, similar initial conditions, along with no interconnection resistances. Such a scenario leads to a uniform current distribution within the parallel cells. However, it is not normally a valid assumption in real world applications. Because for example batteries generate heat during their operation and even with an ideal thermal

management system, there is always some degrees of temperature gradients between the cells. Hence, it leads to a non-uniform SOC and current distribution, resulting different aging rates. This can be more crucial in case of large format batteries with high current flows which generate a higher amount of heat and have a larger surface area. Generally it is difficult to manage the heat from large format batteries very efficiently [18-21]. This part presents the impact of non-identical initial temperatures on the performance of the parallel cells within the (1S 5P) ESS during the constant 3C discharge event. The initial SOC₀ is 1 for all the cells. The temperature discrepancy between the cells is equal to 8°C. In test case 1, the initial temperatures of Cell₁, Cell₂, Cell₃, Cell₄ and Cell₅ are 33°C, 31°C, 29°C, 27°C and 25°C respectively, as shown in Table I. This scenario has been investigated with and without presence of the interconnection resistance (R_{IC}). R_{IC} depends on the cell size, its design and material selection. According to [22] it is typically in the range of 0.08 mΩ – 0.318 mΩ depending on the joining techniques. The nominal cell resistance (R_{cell}), used in this study at 50% SOC is equal to 1.33 mΩ as provided by the manufacturer. A relative R_{IC} to R_{cell} ratio of 1-10% (corresponds to $R_{IC}=0.0133-0.133$ mΩ) was set for the analysis.

Figure 3(a-d) presents the resistance, current, temperature and SOC of each cell within (1S 5P) ESS during the operation for $R_{IC} = 0$. Generally the resistance of the cell is a function of SOC, current and temperature and can be quantified as follows during the operation [14]:

$$R_{cell} = \frac{(OCV - V_t)}{I_{cell}} \quad (7)$$

where OCV is the open circuit voltage, V_t is the terminal voltage, and I_{cell} stands for the cell current. As known, the cell resistance reduces by the temperature. A temperature variation of 8°C resulted in 13% variation between the resistances of the cells. The results show that initially Cell₁, the cell closest to the terminals, draws a higher current, because it is hotter than the other cells. Conversely, Cell₅, the one furthest from the terminal, has a lower temperature, resulting a higher resistance, hence initially it draws the lowest current among the other cells. The current of Cell₁ is 7% higher than the average current and 14% higher than that of Cell₅. After 460 s the currents start to balance until $t=910$ s where the peak load transition occurs between Cell₁ and Cell₅. The transition normally happens through the end of discharge (SOC < 20%), because the cell impedance significantly increases in this region, this has been shown in Figure 3a. The irreversible heat generation of the cell ($Q_{irr,cell}$) is a function of current as described below:

$$Q_{irr,cell} = (OCV - V_t) \times I_{cell} \quad (8)$$

where OCV is the open circuit voltage, V_t denotes the terminal voltage and I_{cell} is the cell current. This equation reveals that the heat, consequently the cell temperature is highly dependent on the current. When the non-uniformity of the currents is higher, a higher temperature variation is observed between the cells. For this case scenario the current variation is not noticeable and the cells temperatures seem to converge by time as the current balance. The initial

temperature variation of 8°C can reach to 3.9°C by the end of discharge. The maximum SOC discrepancy between the cells is observed at $t=840s$, close to the high impedance region. That is because Cell₁ had always the highest current until the peak load transition, hence, the SOC variation accumulated by this point. SOC difference between the cells reached up to 1.2% at the end of discharge.

A low interconnection resistance ($R_{IC}/R_{cell} = 0.01$), doesn't impose significant changes to the performance of the pack, but as R_{IC} increases the deviation amplifies, shown in Figure 4(a-d). Test case 2 is similar to test case 1, but in presence of interconnection resistance, with relative R_{IC} to R_{cell} ratio of 0.1. At $t=0$ there is a 40% difference in the internal resistance of the cells. The initial current drawn by Cell₁ is 1.97 times of the average current and 4.3 times of the lowest current (current drawn by Cell₅). This is because the cells furthest from the terminals encounter a higher interconnection resistance. The current mismatch within the ESS results in 31°C of temperature difference between the cells at the end of discharge. It means that some of the cells might be exposed to a very high temperature, which may impact the safety and reliability of the pack. The capacity loss rate of the pack increases by the temperature variation between the cells. It is recommended to keep the temperature variation between the cells below 5 °C to minimise the capacity loss [23]. The current difference between the cells led to a significant SOC variation of around 52% which can dramatically reduce the driving range and limit the power of the pack.

B. Initial SOC Variation

This section discusses the influence of initial SOC on the overall performance of the cells in the (1S 5P) ESS. In the third case scenario the initial SOC_s for Cell₁, Cell₂, Cell₃, Cell₄ and Cell₅ are 1, 0.98, 0.96, 0.94 and 0.92 respectively and the cells are initially at 25°C, as summarised in Table I. As shown in Figure 5a, the resistance of Cell₁, initially is slightly lower than that of Cell₅, by around 13%. As seen, the difference in the currents is around 62% at the beginning, but they eventually converges. The resulting temperature variation can reach up to 3.6°C which is not noticeable. As the cells become close to the fully discharged state condition, all the parameters converge. Hence, by having 8% SOC inconsistency at the start of the cycle, the cells can still balance under the load. However, it is only valid if the interconnection resistance between the cells is negligible. The performance of the cells for $R_{IC}/R_{cell} = 0.1$ is shown in Figure 6(a-d). The combination of interconnection resistance and SOC variation amplifies the inhomogeneity of the system. An initial resistance variation of 41% is observed between the cells which is significantly high. As a result, Cell₁ carries a significantly higher current, 5 times higher that of the Cell₅. When discharge process of Cell₅ progresses towards the end, the high impedance of the cell compensates for its low interconnection resistance, and the situation is reversed. However the operation time is not enough for the cells parameters to balance. Because the Cell₁ discharges completely, while SOC level of for example Cell₅ is still 49%. The final temperature difference is around 30 °C, which is noticeable. Given that the ideal cell to cell temperature variation is below 5 °C, such a high temperature variation can

drastically reduce the life time of the pack. It is noteworthy that the performance of Cell₃, Cell₄ and Cell₅ is not very different. It reveals that as the number of cells increases to reach the higher capacity for the pack, the inhomogeneity increases. The assumed relative R_{IC} to R_{cell} ratio of 0.1, might be deemed very high, but in case of a faulty interconnection resistance, it can even be higher. Moreover, if the pack is composed of large cells it may cause major safety concerns. As shown in the different case scenarios, R_{IC} has the highest impact on the ESS performance and a high R_{IC} can crucially deteriorate the performance of the ESS.

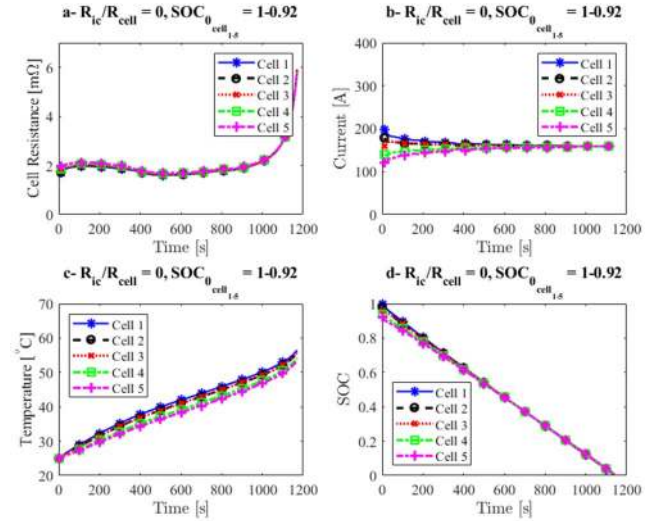


Figure 5. Resistance, current, temperature and SOC of the cells within the (1S 5P) ESS during a constant 3C discharge process due to cell to cell variation of the initial SOC, $R_{IC}/R_{cell} = 0$.

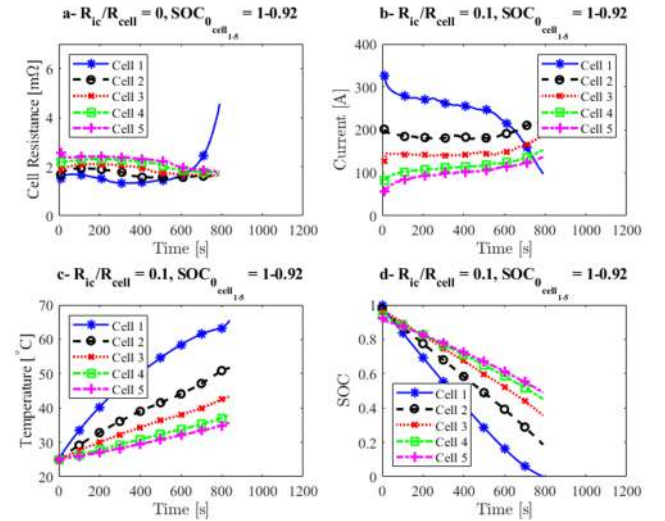


Figure 6. Resistance, current, temperature and SOC of the cells within the (1S 5P) ESS during a constant 3C discharge process due to cell to cell variation of the initial SOC, $R_{IC}/R_{cell} = 0.1$.

VI. FURTHER WORK

The next step of the study will focus on the long term impact of the cell to cell variation on the aging of the pack by quantifying the capacity decay as well as impedance increase. In order to investigate such scenarios, the aging model as well as self-discharge effect will be included in the cell model. Further the system level model will be fully verified by a number of experiments.

VII. CONCLUSION

A validated electrochemical-thermal model of a cell is combined with an electrical model of parallel cells to underpin the performance evaluation of parallel connected cells within the context of a complete ESS. The arrangement of the cells in the ESS is 1S 5P. The impact of interconnection resistance, variation in initial temperature as well as SOC was elaborated in this study. It was found that an initial temperature variation of 8°C between the cells leads to a 14% current variation at $t=0$, along with a maximum of 2.5% SOC variation during the operation. In presence of interconnection resistance the non-uniformity is amplified. It was also observed that a SOC variation of 8% in the initial condition results in 62% variation in the initial currents when there is no interconnection resistance. The results reveal that the interconnection resistance in the primary factor for the inconsistencies and a faulty connection may cause safety concerns especially under high load currents. Such variations not only reduce the EV range, but also result in aging during long term operation. Highly parallelised ESS can amplify the non-uniformity and in case of large format cells the results will be more significant.

ACKNOWLEDGMENT

The research presented within this paper was funded by the Engineering and Physical Sciences Research Council (EPSRC), as a part of ELEVATE project (EP/M009394/1), the Energy Storage SuperGen (EP/L019469/1) in collaboration with the WMG Centre High Value Manufacturing Catapult and Jaguar Land Rover.

REFERENCES

- [1] L. H. Saw, Y. Ye, and A. A. O. Tay, "Integration issues of lithium-ion battery into electric vehicles battery pack," vol. 113, pp. 1032–1045, 2016.
- [2] F. A. Lebel, S. Wilke, B. Schweitzer, M. A. Roux, S. Al-Hallaj, and J. P. F. Trov??o, "A lithium-ion battery electro-thermal model of parallelized cells," *IEEE Vehicular Technology Conference*, pp. 3–8, 2017.
- [3] a a Pesaran, "<Battery thermal models for hybrid vehicle simulations.pdf>," *Journal of Power Sources*, vol. 110, no. 2, pp. 377–382, 2002.
- [4] M. Malik, M., Dincer, I., Rosen, M., Mathew, M., Fowler, "Thermal and electrical performance evaluations of series connected Li-ion batteries in a pack with liquid cooling," *J. Power Sources*, vol. Under Revi, pp. 472–481, 2017.
- [5] T. Baumhöfer, M. Brühl, S. Rothgang, and D. U. Sauer, "Production caused variation in capacity aging trend and correlation to initial cell performance," *Journal of Power Sources*, vol. 247, pp. 332–338, 2014.
- [6] N. Yang, X. Zhang, B. Shang, and G. Li, "Unbalanced discharging and aging due to temperature differences among the cells in a lithium-ion battery pack with parallel combination," *Journal of Power Sources*, vol. 306, pp. 733–741, 2016.
- [7] B. Wu, V. Yufit, M. Marinescu, G. J. Offer, R. F. Martinez-Botas, and N. P. Brandon, "Coupled thermal-electrochemical modelling of uneven heat generation in lithium-ion battery packs," *Journal of Power Sources*, vol. 243, pp. 544–554, 2013.
- [8] T. Bruen and J. Marco, "Modelling and experimental evaluation of parallel connected lithium ion cells for an electric vehicle battery system," *Journal of Power Sources*, vol. 310, pp. 91–101, 2016.
- [9] E. Hosseinzadeh, J. Marco, and P. Jennings, "Electrochemical-Thermal Modelling and Optimisation of Lithium-Ion Battery Design Parameters Using Analysis of Variance," *Energies*, vol. 10, no. 9, p. 1278, 2017.
- [10] E. Hosseinzadeh, J. Marco, and P. Jennings, "The impact of multi-layered porosity distribution on the performance of a lithium ion battery," *Applied Mathematical Modelling*, vol. 61, pp. 107–123, 2018.
- [11] E. Hosseinzadeh, R. Genieser, D. Worwood, A. Barai, J. Marco, and P. Jennings, "A systematic approach for electrochemical-thermal modelling of a large format lithium-ion battery for electric vehicle application," *Journal of Power Sources*, vol. 382, no. November 2017, pp. 77–94, 2018.
- [12] D. Worwood, E. Hosseinzadeh, K. Q. J. Marco, D. Greenwood, M. R. W. . Widanage, A. Barai, and P. Jennings, "Thermal analysis of a lithium-ion pouch cell under aggressive automotive duty cycles with minimal cooling," *IET Hybrid and Electric Vehicles Conference (HEVC 2016)*, pp. 2–3, 2016.
- [13] "Battery cycle life test development for high-performance electric vehicle applications _ Elsevier Enhanced Reader.pdf." .
- [14] E. Hosseinzadeh, J. Marco, and P. Jennings, "Combined electrical and electrochemical-thermal model of parallel connected large format pouch cells," *Journal of Energy Storage*, vol. 22, no. November 2018, pp. 194–207, 2019.
- [15] M. J. Brand, M. H. Hofmann, M. Steinhardt, S. F. Schuster, and A. Jossen, "Current distribution within parallel-connected battery cells," *Journal of Power Sources*, vol. 334, pp. 202–212, 2016.
- [16] S. F. Schuster, M. J. Brand, P. Berg, M. Gleissenberger, and A. Jossen, "Lithium-ion cell-to-cell variation during battery electric vehicle operation," *Journal of Power Sources*, vol. 297, pp. 242–251, 2015.
- [17] S. Paul, C. Diegelmann, H. Kabza, and W. Tillmetz, "Analysis of ageing inhomogeneities in lithium-ion battery systems," *Journal of Power Sources*, vol. 239, pp. 642–650, 2013.
- [18] T. Grandjean, A. Barai, E. Hosseinzadeh, Y. Guo, A. McGordon, and J. Marco, "Large format lithium ion pouch cell full thermal characterisation for improved electric vehicle thermal management," *Journal of Power Sources*, vol. 359, pp. 215–225, 2017.
- [19] E. Hosseinzadeh, A. Barai, J. Marco, and P. Jennings, "A Comparative Study on Different Cooling Strategies for Lithium-Ion Battery Cells," *The European Battery, Hybrid and Fuel Cell Electric Vehicle Congress (EEVC 2017)*, pp. 1–9, 2017.
- [20] D. Worwood, J. Marco, Q. Kellner, E. Hosseinzadeh, R. Mcglen, D. Mullen, K. Lynn, and D. Greenwood, "Experimental Analysis of a Novel Cooling Material for Large Format Automotive Lithium-Ion Cells," 2019.
- [21] D. Worwood, Q. Kellner, D. Greenwood, J. Marco, D. Mullen, and R. M. Glen, "Thermal analysis of fin cooling large format automotive lithium-ion pouch cells," pp. 7–12, 2017.
- [22] M. Baumann, L. Wildfeuer, S. Rohr, and M. Lienkamp, "Parameter variations within Li-Ion battery packs – Theoretical investigations and experimental quanti fi cation," vol. 18, no. April, pp. 295–307, 2018.
- [23] N. Yang, X. Zhang, B. Shang, and G. Li, "Unbalanced discharging and aging due to temperature differences among the cells in a lithium-ion battery pack with parallel combination," *Journal of Power Sources*, vol. 306, pp. 733–741, 2016.